### CONFERENCE PRE-PRINT

# EXPERIMENTAL OBSERVATION OF STREAMER-LIKE STRUCTURE ENHANCING TURBULENT TRANSPORT IN SCRAPE-OFF LAYER OF HL-2A TOKAMAK

J. CHEN

Institute of Fusion Science, School of Physical Science and Technology, Southwest Jiaotong University Chengdu, China

Email: chenjian@my.swjtu.edu.cn

### J. CHENG

Institute of Fusion Science, School of Physical Science and Technology, Southwest Jiaotong University Chengdu, China

Y. XU

Institute of Fusion Science, School of Physical Science and Technology, Southwest Jiaotong University Chengdu, China

N. WU

Southwestern Institute of Physics

Chengdu, China

L.W. YAN

Southwestern Institute of Physics

Chengdu, China

R. KE

Southwestern Institute of Physics

Chengdu, China

Q. ZOU

Institute of Fusion Science, School of Physical Science and Technology, Southwest Jiaotong University Chengdu, China

X. CHEN

Institute of Fusion Science, School of Physical Science and Technology, Southwest Jiaotong University Chengdu, China

J. WEN

Southwestern Institute of Physics

Chengdu, China

Y. YŪ

Sino-French Institute of Nuclear Engineering and Technology, Sun Yat-sen University

Zhuhai, China

Z.H. HUANG

Southwestern Institute of Physics

Chengdu, China

W.C. WANG

Southwestern Institute of Physics

Chengdu, China

Z.B. SHI

Southwestern Institute of Physics

Chengdu, China

X.Q. JI

Southwestern Institute of Physics

Chengdu, China

W.L. ZHONG

Southwestern Institute of Physics

Chengdu, China

M. XU

Institute of Modern Physics, Fudan University

Shanghai, China

# Abstract

A coherent fluctuation with a central frequency around 17.6 kHz has been observed in HL-2A NBI-heated H-mode plasmas. This fluctuation is detected simultaneously in density, floating potential and magnetic signals, implying its electromagnetic properties. Multi-channel beam emission spectroscopy measurements reveal a nearly-zero radial wavenumber and finite poloidal wave number. Bispectral analysis confirms that the fluctuation originates from three-wave nonlinear interactions with background turbulence predominantly in 50–300 kHz range. These features align with theoretically predicted streamers [N. Kasuya et al 2010 Nucl. Fusion 50 054003]. Further analysis shows that the amplitude of these streamer-like structures increases significantly after L-H transition in this discharge scenario, accompanied by a rise in SOL turbulent heat transport including both convective and conductive heat fluxes. This suggests that streamer-like structures could broaden the SOL width while exerting only a minor influence on the L-H transition dynamics. The findings offer a potential strategy for controlling exhaust heat flux while maintaining high plasma performance in future fusion plasmas.

### 1. INTRODUCTION

In future magnetic confinement fusion devices such as ITER, operation in high-confinement mode (H-mode) is expected to improve overall plasma performance, but also poses a serious challenge—the high heat flux load on the divertor targets. Based on the scaling model for the ITER scrape-off layer (SOL) width established by Eich et al., the predicted value of  $\lambda q$  (approximately 1 mm) [1] corresponds to a local heat flux that far exceeds the material limits. Various methods aim to mitigate divertor heat load, including radiative dissipation [2], magnetic configuration optimization [3] and so on. A prominent approach is to broaden the scrape-off layer (SOL) width by enhancing edge and SOL turbulent transport, which has consequently been the subject of extensive research. For instance, in LHD, edge turbulence spreading increase turbulence levels in the stochastic layer and thereby expanding the heat deposition width on the divertor target [4]; In EAST, the spreading of pedestal modes from the pedestal region into the SOL has been observed to increase the divertor particle flux width [5]; Experiments on DIII-D have shown that boundary electron or ion modes can enhance edge turbulent transport, leading to a wider SOL [6].

Notably, drift wave turbulence can excite two key types of secondary flows—zonal flows and streamers—which exert opposing influences on turbulent transport [7,8]. Zonal flows are characterized as nearly axisymmetric (m ≈  $0, n \approx 0$ ) shear flows with a finite radial wavenumber  $(k_r)$  and small poloidal wave numbers  $(k_\theta \approx 0)$ . Zonal flows suppress turbulent transport primarily by generating a sheared E×B flow, which reduces the radial correlation length and coherence of turbulence eddies, thereby weakening cross-field turbulent transport [9]. In contrast, streamers are radially elongated structures with finite poloidal wavenumber  $(k_{\theta})$  and near-zero radial wavenumber  $(k_r \approx 0)$ . General theories and simulations indicate that streamers are generated through nonlinear mode coupling [10,11] or modulational instability of density or temperature gradient-driven instabilities (drift waves) [7,12]. The formation of streamers breaks the symmetry of the turbulence spectrum. Owing to their long radial correlation length, they can markedly enhance turbulent transport, leading to transport coefficients that are often an order of magnitude larger than those predicted by simple mixing-length theory [13]. Consequently, they may increase SOL turbulent transport, thereby broadening the SOL width. Y. Kosuga et al. have theoretically elucidated the scaling relationship of streamers effects on SOL width [14]. Experimental observations of streamer-like or avalanche-like transport phenomena have been reported in several magnetic confinement devices. On DIII-D, avalanche structures exhibiting intermittent transport, 1/f spectral behaviour, and self-similarity—characterized by a Hurst exponent H > 0.5—have been observed, showing clear radial propagation [15]. Similar features have also been identified in KSTAR, JT-60U, and Heliotron J. In KSTAR, interactions between E × B shear flow layers and avalanche-like dynamics have been documented [16]. On JT-60U, avalanche-like events were found to enhance core electron heat transport, contributing up to 10% of the total electron heat flux [17], while also suppressing the formation of internal transport barriers [18]. In Heliotron J, the amplitude of avalanche-like events is observed to depend on the total electron cyclotron heating (ECH) power, with these structures originating in the heated region and propagating radially outward [19]. The other type is streamer structures, which exhibit radial long-range correlation and are generally believed to arise from nonlinear interactions of drift-wave turbulence, possessing a distinct characteristic frequency. These structures characteristics have been observed in LHD [20] and linear devices [21]. Furthermore, streamer-like structures also have been observed in the HL-2A tokamak [22], which has an ability to regulate the distribution of divertor heat flux [22]. However, the underlying physics mechanisms governing the streamer growth, damping and SOL transport following the L-H transition has not yet been fully understood.

This paper reports the observation of streamer-like structures in NBI-heated H-mode plasmas on the HL-2A tokamak. These structures exhibit a finite frequency (f  $\approx$  17.6 kHz), radial long-range correlation ( $k_r \approx 0$ , finite  $k_\theta$ ), and are generated through three-wave nonlinear interactions with background turbulence (in the 50–300 kHz range). They significantly enhance both convective and conductive heat transport in the SOL. The paper is

structured as follows: Section 2 describes the experimental setup; Section 3 presents the experimental results, including features of the streamer-like structures, nonlinear coupling, and analysis of SOL transport; Section 4 provides the summary.

### 2. EXPERIMENTAL SET-UP

The scrape-off layer turbulent transport experiment has been conducted in HL-2A tokamak with a lower single-null divertor structure. The experiment basic parameters are as follows: the line-average electron density  $n_{e,l}$ =

 $(1.7-2.5) \times 10^{19} \text{m}^{-3}$ , plasma current  $I_p = 150-160$  kA, toroidal magnetic field  $B_t = 1.3$  T in the clockwise toroidal direction. The primary heating is neutral beam injection (NBI) and its power is 800 kW. The key diagnostics of the HL-2A tokamak plasma are illustrated in Fig. 1. Fig. 1(a) presents the arrangement of a 24channel beam emission spectroscopy (BES) diagnostic system [23]. Positioned at the low-field-side (LFS) midplane, this system provides two-dimensional measurements of electron density fluctuations spanning from the edge to SOL regions. With a temporal resolution of 0.5 μs, radial resolution <1 cm, and poloidal resolution of 1.2 cm, the BES system enables characterization of turbulent mode structures, determination of radial/poloidal wavenumbers, and investigation of long-range radial correlations. Fig. 1(b) shows a dual-step Langmuir probe array installed on the lower hybrid wave (LHW) antenna [24], which protrudes beyond the first wall to enable measurements in the near scrape-off layer (near-SOL) region. Each step contains four graphite probes: two toroidally aligned probes biased at +180V (labeled V+ and V-) with 8 mm toroidal separation, and two poloidally separated probes (4 mm spacing) measuring floating potentials (V<sub>fl</sub> and V<sub>f2</sub>). Using triple-probe principle [25], local plasma parameters such as electron temperature, electron density, plasma potential, and saturated ion current can be derived. These measurements allow calculation of the SOL particle flux  $\Gamma_r$ =  $\langle \tilde{n}_e \tilde{v}_r \rangle$  and heat flux (including both convective and conductive

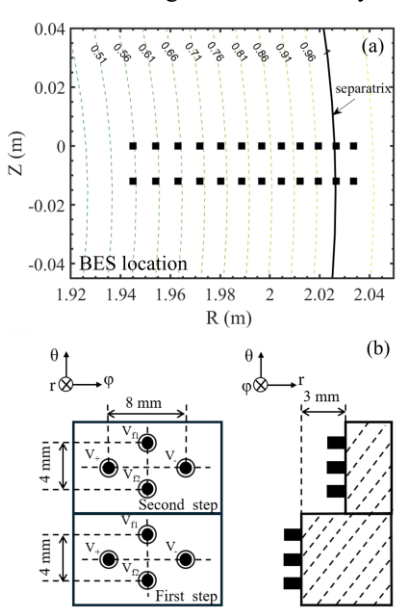


Fig. 1 The measurement locations of the 24-channel BES are overlaid on the magnetic surface (a) and SOL Langmuir probe array installed in LHW antenna (b).

components)  $q_r = \frac{3}{2} \overline{T}_e \langle \tilde{n}_e \tilde{v}_r \rangle + \frac{3}{2} \overline{n}_e \langle \tilde{T}_e \tilde{v}_r \rangle$  with temporal evolution. All Langmuir probe data are acquired at 1 MHz sampling rate with 12-bit digitization, providing comprehensive SOL plasma characterization. The combined diagnostics offer different spatial measurements for microscopic turbulence, facilitating relevant studies of SOL transport physics and edge turbulence transport characteristics in HL-2A tokamak.

### 3. EXPERIMENTAL RESULTS

# 3.1. The temporal evolution of fundamental plasma parameters.

Fig. 2 presents the temporal evolution of key plasma parameters during the L-H transition and subsequent H-mode phase in HL-2A. Fig. 2(a) displays the lineaveraged electron density (n<sub>e,l</sub>) and plasma current (I<sub>p</sub>) waveforms, showing characteristic density buildup following the transition. Fig. 2(b) illustrates the neutral injection (NBI) heating power, with approximately 700 kW of auxiliary power applied at t = 800 ms to facilitate the transition. The confinement characteristics are quantified in Fig. 2(c) through the  $H_{98}$  confinement factor  $(H_{98} \equiv \tau_E/\tau_{ITER98(y,2))}$  and normalized beta  $(\beta_N \equiv \beta(\%) \cdot a(m) \cdot B_0(T)/I_p(MA)),$ where  $\beta$  is the beta, a is the minor radius, and  $B_0$  the toroidal field. A clear improvement in confinement is observed post-transition, with  $H_{98}$  reaching 1-2 and  $\beta_N$ stabilizing at 2-2.5, indicating operation in the highbeta regime. Fig. 2(d) shows the  $D_{\alpha}$  emission signal,

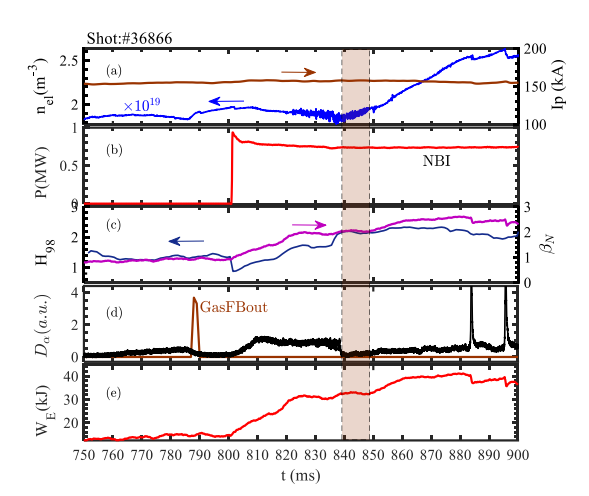


Fig. 2 Time evolution of (a) line-average electron density  $(n_{e,l})$  and plasma current  $(I_p)$ ; (b) the NBI injection power; (c) the confinement factor  $(H_{98})$  and normalized beta  $(\beta_N)$ ; (d) the  $D_\alpha$  emission and feedback-controlled gas injection; (e) the plasma stored energy  $(W_E)$ .

where the characteristic reduction at t = 840 ms marks the L-H transition, followed by the appearance of edge-localized modes (ELMs). The brown shaded region highlights the time window of primary interest for this study, encompassing the transition phase and early H-mode period.

Fig. 3 presents a detailed investigation of coherent mode (CM) characteristics after the L-H transition in HL-2A tokamak. Fig. 3(a) shows the  $D_{\alpha}$  emission evolution, clearly marking the transition to H-mode at t=840 ms. The BES measurements in Fig. 3(b) and Fig. 3(c) reveal distinct density fluctuation time-frequency spectra at the edge ( $\rho$ ~0.93) and separatrix ( $\rho$ ~1.00) regions, respectively. A well-defined coherent mode emerges during the transition phase (t = 820-850 ms) with a characteristic frequency of 17.6 kHz, exhibiting both electrostatic and electromagnetic characteristics as confirmed by correlated magnetic probe signals. These fluctuations in SOL ( $\rho$  = 1.15) are comprehensively characterized through Langmuir probe measurements of electron temperature ( $T_e$ ), and radial velocity ( $v_r$ ) perturbations, shown in Fig. 3(d)-(e). During L-mode, the CM remains weakly localized in the confined region with minimal SOL response. Following the transition to H-mode, the mode amplitude increases substantially and its influence becomes clearly observable across all measured SOL parameters. The coherent 17.6 kHz modulation appears simultaneously in  $T_e$ , and  $v_r$  fluctuations, demonstrating significant penetration into the SOL region. These observations suggest that the CM may play an important role in mediating SOL transport during H-mode. Meanwhile, these findings provide new evidence for non-local coupling between edge and SOL dynamics in H-mode plasma. The detailed mechanisms of CM-driven transport and their quantitative impact on SOL transport will be further examined in subsequent analysis.

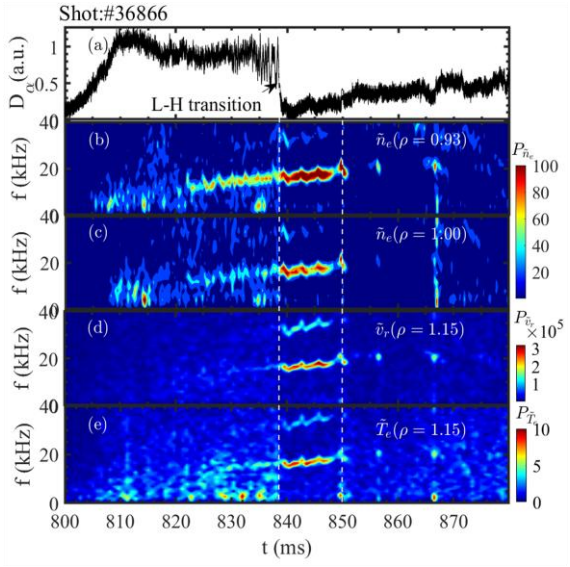


Fig. 3 Time history of the  $D_a$  emission (a); the time-frequency spectra of electron density fluctuation in edge (b) and separatrix (c); the time-frequency spectra of electron temperature (d) and radial velocity fluctuation (e) in SOL.

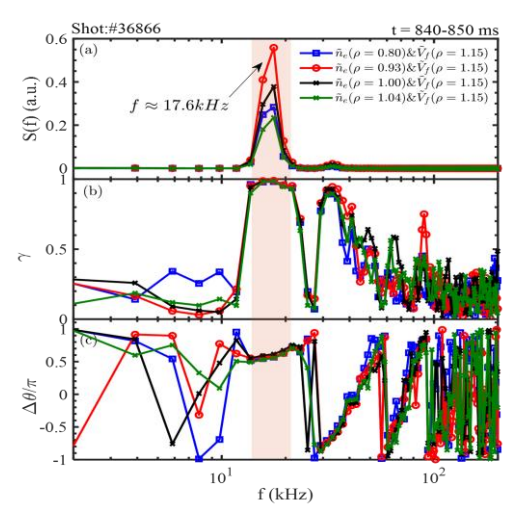


Fig.4 The cross-spectral analyses between electron density fluctuations at normalized radius  $\rho=0.8$  (core), 0.93 (edge), 1 (separatrix), and 1.04 (SOL), and floating potential fluctuations in the SOL region ( $\rho=1.15$ ): cross-power spectrum(a), cross-coherence spectrum (b), and cross-phase spectrum(c).

# 3.2. Radial long-range correlation characteristics and their generation mechanisms.

The radial correlation properties of the 17.6 kHz CM have been thoroughly investigated through cross-spectral analysis between density fluctuations measured by BES at multiple radial locations and floating potential fluctuations from SOL Langmuir probes. Fig. 4 presents the cross-power spectrum (a), coherence spectrum (b), and cross-phase spectrum (c) for four representative radial positions:  $\rho$ ~0.8 (core),  $\rho$ ~0.93 (edge),  $\rho$ ~1 (separatrix), and  $\rho$ ~1.04 (near-SOL). The cross-power spectra reveal a distinct peak at  $f_{CM}\approx17.6$  kHz across all analyzed positions, demonstrating the CM existence throughout the edge and SOL regions. The high coherence ( $\gamma$ >0.8) at this frequency confirms the CM radial long-range correlation, with an estimated correlation length of ~9 cm. The cross-phase analysis shows a remarkably constant phase difference ( $\Delta\Phi\approx0.6\pi$ ) between density and potential fluctuations at  $f_{CM}$ , indicating the CM maintains phase coherence without exhibiting radial propagation characteristics. These observations suggest the CM represents a globally coherent structure. The CM extended correlation length and stationary phase relationship have significant implications for understanding cross-field transport processes in H-mode plasmas. To further verify the radial long-range correlation characteristics of this structure, we performed two-point correlation analysis [26] on BES signals from radially separated channels  $\Delta$ r = 6.54 cm and poloidally separated channels  $\Delta$ 0 = 1.2 cm near  $\rho$ <0.97. Fig. 5(a)-(b) presents the resulting poloidal

and radial wavenumber spectra obtained through this analysis. The poloidal wavenumber spectrum in Fig. 5(a) reveals a distinct peak at  $f\approx 17.6$  kHz with <k $_{\theta}>\approx 0.25$  cm $^{-1}$ , while the corresponding radial wavenumber spectrum in Fig. 5(b) shows <k $_{r}>\approx 0$  cm $^{-1}$  at the same frequency. Thus, the wavenumber-frequency spectrum provides additional evidence that the CM exhibit long-range radial correlations.

To investigate the generation mechanism of CM, bispectral analysis has been employed to characterize the nonlinear three-wave coupling processes in the SOL [27]. This technique has been widely applied in plasma turbulence studies to identify phase-coupled interactions between different frequency components. The squared auto-bicoherence is calculated as:

$$b^{2}(f_{1}, f_{2}) = \frac{|B(f_{1}, f_{2})|^{2}}{\langle |X(f_{1})X(f_{2})|^{2} \rangle \langle |X(f_{3})X^{*}(f_{3})|^{2} \rangle}$$
(1)

where the bispectrum  $B(f_1, f_2)$  is defined as:

$$B(f_1, f_2) = X(f_1)X(f_2)X^*(f_1 \pm f_2) = \frac{1}{N} \sum_{i=1}^{N} X(f_1)X(f_2)X^*(f_1 \pm f_2)$$
 (2)

Here, X(f) represents the Fourier transform of the time series x(t), the asterisk (\*) denotes complex conjugation, and N corresponds to the ensemble number used for statistical averaging. The angular brackets  $\langle \rangle$  indicate ensemble averaging over multiple realizations of the turbulent fluctuations. The frequency sum

rule  $f_3 = f_1 + f_2$  satisfies the wave-wave coupling condition for nonlinear interactions in plasma turbulence. In this work, bi-spectrum analysis is performed using floating potential fluctuations, measured by Langmuir probes in the SOL region, the results of which are shown in Fig. 5 (c)-(d). The squared auto-bispectrum analysis displayed in Fig. 5(c) with color-coded coupling strength, reveals significantly enhanced  $b^2(f_1,f_2)$  at frequency combinations ( $f_2 = \pm 17.6 \text{ kHz}$  and sum frequency  $f = f_1+f_2 = 17.6$  kHz), demonstrating strong three-wave coupling in the 50-300 kHz turbulence spectrum. More details can be seen from the enlarged view of Fig. 5(c). The summed bispectrum b2(f) in Fig. 5(d) exhibits a dominant spectral peak centered at 17.6 kHz, providing compelling evidence that the CM generation mechanism is efficient energy transfer via nonlinear interactions between CM and background turbulence. Similar three-wave coupling has also been observed in SOL turbulence on the W7-X stellarator [28]. These observations confirm that significant three-wave nonlinear interactions can occur in the SOL region as well. These features of limited poloidal wavenumber and near-zero radial wavenumber, generated through nonlinear process,

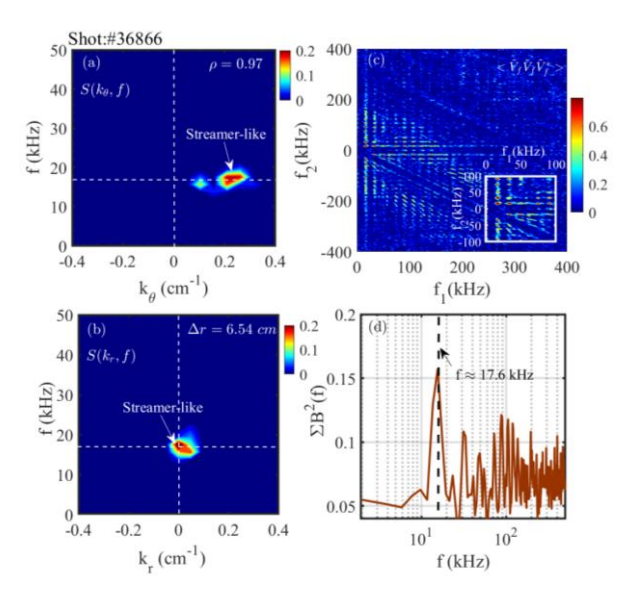


Fig. 5 Wavenumber-frequency spectrum  $S(k_{\theta}, f)$  of electron density fluctuations measured at two poloidally separated locations ( $\Delta\theta = 1.2$  cm) (a). Corresponding spectrum for radially separated measurements ( $\Delta r = 6.54$  cm) (b). Contour plot of squared auto-bicoherence for floating potential fluctuations in the SOL region(c). Frequency-dependent summed bicoherence  $\sum b^2(f)$  (d).

provide direct evidence that the observed CM exhibit the streamer structures predicted by theoretical and simulations. Based on these definitive wavenumber characteristics, we hereafter refer to this CM as a "streamer-like structures", emphasizing its correspondence with theoretical predictions of streamer formations in magnetically confined plasmas [29].

# 3.3 Dynamics of streamer-like structures after L-H transition

According to the above described as shown in Figs. 3 (b)-(d), it is found that the amplitude of streamer-like structures significantly increases after the L-H transition where the E×B shear flow is very strong, indicating that this streamer-like structure plays a negligible role in the plasma confinement. To study the streamer dynamic behaviors, it is necessary to analyze the driving and damping processes of streamers. Theoretically, the formation of streamers originates from the modulational instability of drift waves turbulence. In the absence of zonal flows, a predator—prey model describing the interaction between drift waves and streamers is derived from the wave kinetic equations, as follows [30]:

$$\frac{\partial W}{\partial t} = \gamma_{eff} W - \alpha W S \left( 1 - \frac{k_{\perp}^2 V_d^2 S}{\gamma_{NS}^2 W} \right) \tag{3}$$

$$\frac{\partial S}{\partial t} = \alpha W S \left( 1 - \frac{k_{\perp}^2 V_d^2 S}{V_{NS}^2 W} \right) - \gamma_S S \tag{4}$$

Here, W and S represent the energy of drift waves and streamers, respectively;  $\gamma_{\rm eff}$  is the effective growth rate of drift waves;  $\gamma_S$  denotes the damping rate of streamers; and the nonlinear term  $\alpha WS \left(1 - \frac{k_\perp^2 V_d^2 S}{\gamma_{NS}^2 W}\right)$  represents the energy transfer from drift waves to streamers. This model predicts a threshold condition for streamer excitation

or suppression, namely  $\frac{\gamma_s \omega_*}{\gamma_L \alpha} \sim O(1)$ . Using discharge parameters from HL-2A #36866, this critical condition is satisfied, indicating that streamers can be either excited or suppressed under the given parameters. To further evaluate the relative strength of streamer drive versus flow shear, the conditionally averaged waveform of the streamer is obtained [31]. During the decay phase of the waveform, where the driving term is assumed negligible, an exponential fit is applied to the trailing edge,  $S=S_0e^{-\mu t}$  yielding the damping rate  $\mu$ . The evolution equation for the streamer energy can then be simplified as  $\frac{\partial S}{\partial t} = \gamma_{drive} S - \mu S$ . Dividing both sides by S, we obtain  $\gamma = \gamma_{drive} - \mu$ , where  $\gamma = \frac{1}{S} \frac{dS}{dt}$  is the instantaneous growth rate of the streamer. The drive rate for the streamer is thus derived as  $\gamma_{\text{drive}} = \gamma + \mu$ . As shown in Fig. 6(a), the conditionally averaged streamer-like structures amplitude (blue curve) and its time derivative dS/dt (black curve) are presented. Normalizing the latter yields  $\frac{1}{s} \frac{ds}{dt}$ . An exponential fit to the trailing edge gives a damping rate of  $\mu$ =2.43×10<sup>5</sup> s<sup>-1</sup>. The resulting drive rate  $\gamma_{\text{drive}}$  is shown in Fig. 6(b), where the red shaded area indicates the range of the  $E \times B$  shearing rate in HL-2A typical H-mode discharges [32]. The results demonstrate that the drive rate exceeds

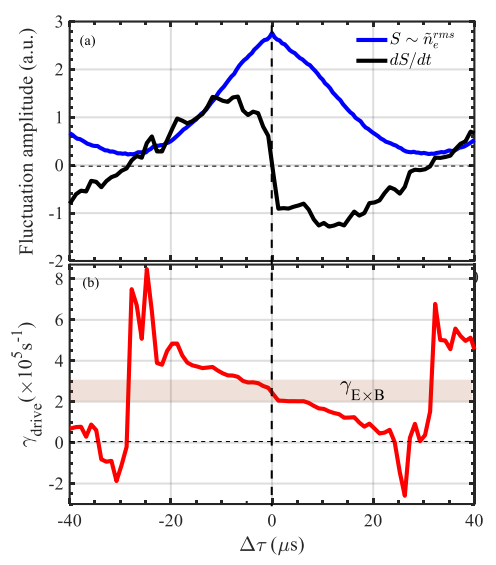


Fig. 6. The auto conditionally-averaged waveform of density fluctuation measured at  $\rho \approx 0.93$ , alongside dS/dt (a), as well as the derived turbulence-driving rate  $\gamma_{drive}$  (b). The shaded areas denote the  $E \times B$  shear rate ranges in H-mode.

the  $E \times B$  shearing rate during the streamer-like structures growth phase. This indicates that even with enhanced flow shear in H-mode, streamer-like structures can still be driven and sustained when the drive is sufficiently strong. These findings support the plausibility of streamer existence in H-mode plasmas.

### 3.4 The contribution from streamer to cross-field heat flux in SOL

While theoretical models predict that streamer structures significantly enhance turbulent transport in the SOL, experimental verification of their modulation effects has remained elusive. This work presents comprehensive measurements of streamer-like impact on SOL and divertor target heat fluxes. Fig. 7(a) displays the temporal evolution of floating potential fluctuations in the SOL region, with shaded intervals clearly indicating periods of enhanced streamer-like structures. To quantify the relative contributions of convective versus conductive transport, we analyse the SOL heat flux  $q_r = \frac{3}{2} \bar{T}_e \langle \tilde{n}_e \tilde{v}_r \rangle + \frac{3}{2} \bar{n}_e \langle \tilde{T}_e \tilde{v}_r \rangle$ , normalized by  $\bar{n}_e \bar{T}_e$  to yield  $q_{(r,norm)} = \frac{3}{2} \langle \tilde{n}_e / \bar{n}_e \tilde{v}_r \rangle + \frac{3}{2} \langle \tilde{T}_e / \bar{T}_e \tilde{v}_r \rangle$ , where the first and second terms corresponding to normalized convective and conductive components, respectively [33]. As shown in Fig. 7(b), streamer-like structures lead to comparable enhancement in both transport channels. To further verify that the observed heat transport enhancement is indeed caused by streamer-like structures, we perform Fourier decomposition of the aforementioned normalized heat flux. The expression is

$$q(f) = \frac{3}{2} \gamma_{(\tilde{n}_e/\bar{n}_e,\tilde{v}_r)}(f) \sqrt{P_{\tilde{n}_e/\bar{n}_e}(f)P_{\tilde{v}_r}(f)} cos\theta_{(\tilde{n}_e/\bar{n}_e,\tilde{v}_r)}(f) + \frac{3}{2} \gamma_{(\bar{T}_e/\bar{T}_e,\tilde{v}_r)}(f) \sqrt{P_{\bar{T}_e/\bar{T}_e}(f)P_{\tilde{v}_r}(f)} cos\theta_{(\bar{T}_e/\bar{T}_e,\tilde{v}_r)}(f)$$
(5)

where P representing the auto-power spectrum,  $\alpha$  denoting the cross-phase, and  $\gamma$  signifying the cross-coherence. Fig. 7(c)-(g) present the auto-power spectra of relative density  $(\tilde{n}_e/\bar{n}_e)$  and temperature  $(\tilde{T}_e/\bar{T}_e)$  fluctuations (c), radial velocity fluctuations  $\tilde{v}_r$  (d), their cross-coherence (e) and phase (f), and the frequency-resolved heat flux

components (g). Distinct spectral peaks at f~17.6 kHz appear consistently across all measurements, with cross-phase cosines 1 confirming synchronous modulation of density/temperature and radial velocity fluctuations, while the frequency-resolved heat flux spectra reveal nearly identical peaks for both convective and conductive components. Together, these observations provide definitive experimental evidence that streamer-like structures comparably enhance both forms of heat transport in the SOL.

### 4. SUMMARY

In summary, streamer-like structures at a central frequency of 17.6 kHz has been observed in HL-2A tokamak H-mode plasma. This structure is observed in density, floating potential and magnetic signals, indicating its electromagnetic characteristics. Multichannel BES measurements indicate streamer-like structures have wavenumber-frequency spectra with  $k_r \approx 0$  and finite  $k_\theta$ . Bispectral analysis demonstrates their generation through three-wave nonlinear interactions with background turbulence in the 50-300 kHz range. These observed characteristics are in agreement with the theoretically-predicted streamers. Our experimental findings demonstrate that the streamer-like structures could enhance SOL heat transport while having a minor influence on L-H transition. The study provides a new insight for

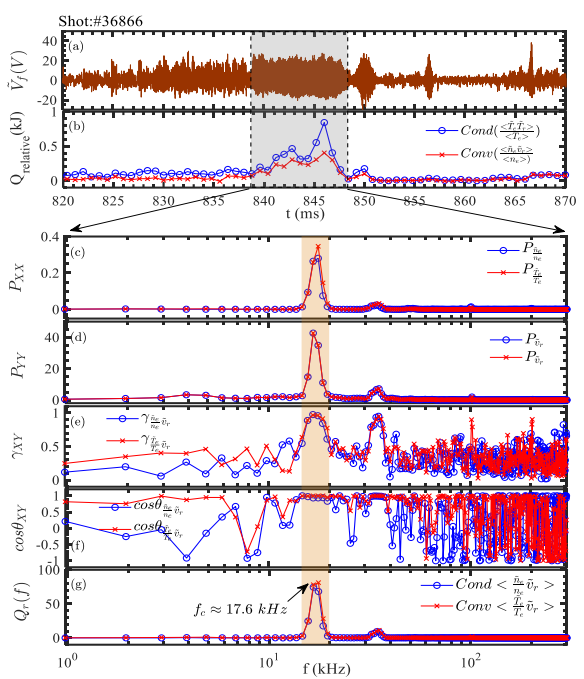


Fig. 7 (a) Time evolution of floating potential fluctuations in near-SOL region; (b) normalized convective and conductive heat flux components. The decomposed heat flux components in the frequency range in SOL: (c) the auto-power spectra of  $\tilde{n}_e/n_e$  and  $\tilde{T}_e/T_e$ , (d) the auto-power spectra of  $\tilde{v}_r$ , (e) the coherence and (f) cosine value of the phase shift between  $\tilde{n}_e/n_e$  ( $\tilde{T}_e/T_e$ ) and  $\tilde{v}_r$ , and (g) decomposed frequency-dependent convective and conductive heat flux contributions.

controlling SOL heat flux and the related width while maintaining high plasma performance in future fusion plasmas.

### **ACKNOWLEDGEMENTS**

We are grateful to Prof. K. Itoh, Prof. J. Q. Dong, and Prof. S. J. Wang for their insightful discussions. This research received funding from multiple sources, including the National Science Foundation of China (Grant Nos. 12175186, 12475219, and U22A20262), the National MCF Energy R&D Program of China (Grant Nos. 2022YFE03070001, 2019YFE03040002, and 2019YFE03030002), and the Sichuan Science and Technology Program (Grant No. 2025ZNSFSC0066).

### REFERENCES

- [1] EICH, T., LEONARD, A.W., PITTS, R.A., et al., Scaling of the tokamak near the scrape-off layer H-mode power width and implications for ITER, Nucl. Fusion 53 (2013) 093031
- [2] LI, K.D., XU, G.S., YANG, Z.S., et al., Divertor detachment with neon seeding in grassy-ELM H-mode in EAST, Plasma Phys. Control. Fusion 62 (2020) 095025
- [3] RYUTOV, D.D., COHEN, R.H., ROGNLIEN, T.D., et al., A snowflake divertor: a possible solution to the power exhaust problem for tokamaks, Plasma Phys. Control. Fusion 54 (2012) 124050
- [4] KOBAYASHI, M., TANAKA, K., IDA, K., et al., Turbulence spreading into an edge stochastic magnetic layer induced by magnetic fluctuation and its impact on divertor heat load, Phys. Rev. Lett. 128 (2022), 125001
- [5] ZHANG, T., LONG, F.F., LI, G.S., et al., Observation of pedestal mode spreading into SOL and broadening of divertor particle flux width on EAST tokamak, Nucl. Fusion 65 (2025) 056019
- [6] ERNST, D.R., BORTOLON, A., CHANG, C.S., et al., Broadening of the divertor heat flux profile in high confinement tokamak fusion plasmas with edge pedestals limited by turbulence in DIII-D, Phys. Rev. Lett. 132 (2024) 235102
- [7] CHAMPEAUX, S., DIAMOND, P.H., Streamer and zonal flow generation from envelope modulations in drift wave turbulence, Phys. Lett. A 288 (2001) 214

- [8] DAS, A., SEN, A., MAHAJAN, S., KAW, P., Zonal and streamer structures in magnetic-curvature-driven Rayleigh -Taylor instability, Phys. Plasmas, 8 (2001) 5104
- DIAMOND, P.H., ITOH, S-I., ITOH, K. ET AL., Zonal flows in plasma—a review, Plasma Phys. Control. Fusion 47 (2005) R35
- [10] BEYER, P., BENKADDA, S., Nondiffusive Transport in Tokamaks: Three-Dimensional Structure of Bursts and the Role of Zonal Flows, Phys. Rev. Lett. 85 (2000) 4892
- [11] KASUYA, N., YAGI, M., ITOH, K., et al., Selective formation of turbulent structures in magnetized cylindrical plasmas, Phys. Plasmas, 15 (2008) 052302
- [12] GURCAN, O.D., DIAMOND, P.H., Streamer formation and collapse in electron temperature gradient driven turbulence, Phys. Plasmas, 11 (2004) 572
- [13] DRAKE, J.F., GUZDAR, P.N., HASSAM, A.B, Streamer formation in plasma with a temperature gradient, Phys. Rev. Lett. 61 (1988) 2205
- [14] KOSUGA, Y., KIN, F., SASAKI, M., Scrape-off layer width set by non-linear streamer flows in drift wave turbulence, Contrib. Plasma Phys. 60 (2020) e201900141
- [15] POLITZER, P.A., Observation of Avalanche-like Phenomena in a Magnetically Confined Plasma, Phys. Rev. Lett. 84 (2000) 1192
- [16] CHOI, M.J., JHANG, H., KWON, J.M., et al., Experimental observation of the non-diffusive avalanche-like electron heat transport events and their dynamical interaction with the shear flow structure, Nucl. Fusion 59 (2019) 086027
- [17] KIN, F., ITOH, K., BANDO, T., et al., Experimental evaluation of avalanche type of electron heat transport in magnetic confinement plasmas, Nucl. Fusion 63 (2023) 016015
- [18] KIN, F., ITOH, K., BANDO, T., et al., Impact of avalanche type of transport on internal transport barrier formation in tokamak plasmas, Sci. Rep., 13 (2023) 19748
- [19] KIN, F., INAGAKI, S., NAGASAKI, K., et al., Observation of avalanche-like transport in Heliotron J and JT-60U plasmas, Nucl. Fusion 64 (2024) 066023
- [20] INAGAKI, S., TOKUZAWA, T., ITOH, K., et al., Observation of long-distance radial correlation in toroidal plasma turbulence, Phys. Rev. Lett., 107 (2011) 115001
- [21] YAMADA, T., ITOH, S-I., MARUTA, T., et al., Anatomy of plasma turbulence, Nat. Phys., 4 (2008) 721
- [22] CHEN, J., CHENG, J., XU, Y., et al., Observation of divertor heat flux regulation by the streamer-like structures in HL-2A NBI-heated H-mode plasmas, Nucl. Fusion (2025) in press
- [23] KE, R., WU, Y.F., MCKEE, G.R., et al., Initial beam emission spectroscopy diagnostic system on HL-2A tokamak, Rev. Sci. Instrum., 89 (2018) 10D122
- [24] XIAO, G.L., ZHONG, W.L., ZOU, X.L., et al., Effect of lower hybrid current drive on pedestal instabilities in the HL-2A tokamak, Phys. Plasmas 24 (2017) 122507
- [25] CHEN, S-L., SEKIGUCHI, T., Instantaneous direct-display system of plasma parameters by means of triple probe, J. Appl. Phys. 36 (1965) 2363
- [26] BEALL, J.M., KIM, Y.C., POWERS, E.J., et al., Estimation of wavenumber and frequency spectra using fixed probe pairs, J. Appl. Phys. 53 (1982) 3933
- [27] KIM, Y.C., POWERS, E.J., Digital bispectral analysis and its applications to nonlinear wave interactions, IEEE Trans. Plasma Sci. 7 (1979) 120
- [28] XIANG, H.M., KRÄMER-FLECKEN, A., HAN, X., et al., Investigation of a low frequency coherent mode in Wendelstein 7-X with island divertor, Nucl. Fusion 63 (2023) 126050
- [29] KASUYA, N., YAGI, M., ITOH, K., et al., Selective formation of streamers in magnetized cylindrical plasmas, Nucl. Fusion 50 (2010) 054003
- [30] ITOH, S-I., ITOH, K., Possible maximum amplitude of streamers in drift wave turbulence, Plasma Phys. Control. Fusion 50 (2008) 055002
- [31] ALONSO, J.A., HIDALGO, C., PEDROSA, M.A., et al., Dynamic transport regulation by zonal flow-like structures in the TJ-II stellarator, Nucl. Fusion 52 (2012) 063010
- [32] WEN, J., SHI, Z.B., ZHONG, W.L., et al., Effects of inter-ELM quasi-coherent modes on the dynamics of pedestal turbulence on HL-2A tokamak, Nucl. Fusion 64 (2024) 076054
- [33] WHITE, A.E., SCHMITZ, L., MCKEE, G.R., et al., Measurements of core electron temperature and density fluctuations in DIII-D and comparison to nonlinear gyrokinetic simulations, Phys. Plasmas, 15 (2008) 056116